Pergamon

Int. J. Multiphase Flow Vol. 24, No. 3, pp. 453–478, 1998

Printed in Great Britain
PII: S0301-9322(97)00053-0
0301-9322/98 $19.00 + 0.00

ASYMPTOTIC ANALYSIS OF VORTEX FLOWS IN SUSPENSIONS

R. PRUD'HOMME[1], L. GOTTESDIENER[1], E. DODEMAND[2] and P. KUENTZMANN[3]

[1]Laboratoire de modélisation en mécanique, Université P. et M. Curie, 4 place Jussieu, 75252 Paris, Cedex 05, France
[2]16 rue Dagorno, 75102 Paris, France
[3]Office National d'Etudes et de Recherches Aérospatiales, 29 Avenue de la Division Leclerc, 92320 Chatillon, France

(Received 1 July 1996; in revised form 11 July 1997)

Abstract—The velocity and concentration fields of two-phase vortex flows have been studied. Analytical methods were used where possible to solve a number of particularly simple cases easy to be interpreted physically. Two cases of gaseous motion were considered: the vortex with concentrated vorticity and the Rankine vortex. For each vortex, the motion of one particle was studied at first, using an asymptotic multiple scales method, and the results were compared with numerical data. Then an equivalent particle continuum was analyzed, first in terms of Lagrangian coordinates, then in Eulerian variables, assuming the time dependent or stationary solutions to be rotationally invariant. © 1998 Elsevier Science Ltd. All rights reserved

Key Words: multiphase flow, suspension, vortex, asymptotic method, multiple scale method

1. INTRODUCTION

Fluid flows often exhibit vortices. Vortices are encountered, for instance, in cloudbursts and cyclones and—on a completely different scale—in superfluid helium. This type of phenomenon also occurs when draining vessels (Guyon *et al.* 1991). In other cases, vorticity may not be as concentrated, but rotating flow structures still exist. This is the case for shear layers or mixing layers between fluids moving at different velocities. Periodic shedding of coherent vortex structures can also be observed in the wakes of obstacles. In the vicinity of sharp edges, such as the case of an aircraft wing trailing edge, areas of very high velocity exist. These high velocities give rise to a highly vortical motion that is then carried away by the flow (Germain 1986). These vortices can be stretched and sometimes they split and tend rapidly towards disorder and dissipation (Delery *et al.* 1997). Finally, structures of this type are also visible in Jupiter's atmosphere on a scale of several tens of thousands of kilometers. These vortex regions of varying vorticity appear clearly during numerical simulations based on well-known systems of equations. The case of a two-dimensional vortex with concentrated vorticity in a single phase fluid is well-known. Such a fluid vortex is also called an irrotational vortex since outside its center, considered as a singularity, the flow is irrotational and circulation of the velocity vector on any closed curve containing the center is constant and equal to Γ. This vortex can be dissipated by viscosity in a medium remaining at rest at infinity (Germain 1962). Growth of a quasi-solid core of radius $r \approx \sqrt{\nu t}$ can be observed. The rate of expansion of the core decreases as $\Gamma/\nu t$ such that, asymptotically, the vortex structure includes this central core surrounded by the initial irrotational vortex. Marble (1985, 1988) investigated the development of vortices in presence of chemical reactions with unmixed, then premixed species. He demonstrated that, in certain cases, the growth of a mixing core resulting from diffusion and combustion is observed in addition to the quasi-solid core.

There are fewer models for flows with particles than for one phase fluids (Fortier 1967; Kuentzmann 1973; Clift *et al.* 1978; Soo 1990; Nigmatulin 1991). This is why it was interesting to solve, analytically where possible, a number of particularly simple cases easy to interpret phy-

sically. From the results obtained, one will infer a few characteristics of the laminar behavior of suspensions in vortex flows. These results may be useful for the experimentalist (problems of flow seeding for laser anemometry measurement), for the computational specialist and for the engineer facing industrial multiphase flow problems. It should be noted that we only investigated rotationally invariant flows as will be mentioned.

Three types of vortices are considered: the vortex with vorticity concentrated at a point (irrotational vortex), the Rankine vortex and the modified Rankine vortex.

For the irrotational vortex, an analytical approach shall be tried, be it only by determining asymptotic solutions. In other cases, numerical analysis will provide a complete solution.

First of all, before discussing the behavior of a suspension which is a so-called particle-continuum, we must clearly recall the assumptions made for a particle of this suspension and describe how the equations are to be used. The particles investigated are assumed to be spherical, the force acting on them by the surrounding gas is given by Stokes' theory and that there are no heat or mass transfer between the particles and the gas.

The problem of the influence of other forces was investigated by several authors in different situations such as the propagation of small periodic perturbations (Dodemand *et al.* 1995), and the effect of vortex motion (Tio *et al.* 1993a,b) with or without heat or mass transfer. The influence of gravity has been investigated, over the last few years, in particular by Gañán-Calvo and Lasheras (1991); Tio *et al.* (1993a,b); Lasheras and Tio (1994). These authors have found several stable and unstable structures, closed orbits and attractors for particles whose specific density is generally larger than the fluid density.

Marcu *et al.* (1995) have studied the effect of gravity on particles which move inside a Burgers vortex. Burgers vortex-like structures seem to be preeminent in turbulence. In the case of zero gravity there exist a critical value of the Stokes number under which the particle is driven by the flow towards the center of the vortex. Gravity effects lead to more complex situations and one or three equilibrium points appear away from the center depending on the Stokes and Froude numbers. Studying the vicinity of these equilibrium points one observes changes in stability as functions of terminal velocity and strain parameter. Nodes, focuses, closed trajectories and saddle points are obtained.

It is assumed, in these studies, that the condensed particles do not disturb the fluid motion and are only influenced by it. A discussion about the relative importance of the different terms is presented at the end of this paper (see Appendix A).

The analysis is limited to the simplest case, in order to thoroughly investigate the asymptotic behavior of a case that remains realistic. Since the fluid motion was given by the velocity field $\boldsymbol{v_g}$, the following vector equation should be solved:

$$\frac{d_p \mathbf{v}_p}{\mathrm{d}t} = \frac{\mathbf{v}_g - \mathbf{v}_p}{\tau_v} \qquad [1]$$

where $\mathbf{v}_p$ is the particle velocity, $(d_p \mathbf{v}_p)/(\mathrm{d}t)$ the particle acceleration and τ_v the particle/gas relaxation time which is assumed to be constant (see Appendix A).

The particle trajectories will be determined, as the motion in planes (x,y) or (r,t) and (θ,t) or (r,v_{pr}) and $(r,v_{p\theta})$ or again (r,θ), preferably after having made the terms of equation dimensionless. The analysis of particle motion in a force field is nothing new for those who study mechanics or particle physics, continually confronted with this type of problem. The present work focuses on vortex movements and solutions of, in view of applying the results to the study of suspensions.

The problems raised at the particle continuum scale are multiple. (We consider this a macroscopic scale as opposed to the microscopic scale of the particle and the molecular scale internal to the particle or gas.)

First the velocity field will be investigated. It can be defined in Eulerian coordinates or Lagrangian coordinates. In the case of suspensions of uniform concentration at $t = 0$, some very simple and characteristic situations are of great interest in understanding the phenomenology of the motion. Generally, Eulerian coordinates can then be used to clearly define what is understood by a rotationally invariant solution near the center of the vortex and by a steady or

unsteady solution. These results have to be converted to Lagrangian coordinates to take advantage of the knowledge gained from the analysis of the motion of an isolated particle.

In addition, questions will be asked concerning the continuity of the solutions and the physical assumptions to be made concerning the continuum approach.

In cylindrical (or two-dimensional polar) Eulerian coordinates, it is always assumed that the radial and angular components of the velocity vector depend only on the radial coordinate r and the time (velocity field invariant by rotation at time t):

$$v_{pr} = v_{pr}(r,t),\ v_{p\theta} = v_{p\theta}(r,t). \qquad [2]$$

In Lagrangian coordinates, due to the rotation invariance of the initial positions, it can be written:

$$r = r(a,\tau),\ a = r(a,0),\ t = \tau,\ \mathrm{d}r = \frac{\partial r}{\partial a}\mathrm{d}a + \frac{\partial r}{\partial \tau}\mathrm{d}\tau,\ \mathrm{d}t = \mathrm{d}\tau,$$

i.e. by inversion:

$$\mathrm{d}a = \frac{\mathrm{d}r - (\partial r/\partial \tau)\mathrm{d}t}{\partial r/\partial a}.$$

Then the Eulerian partial derivatives $\partial v_r/\partial t$, $\partial v_\theta/\partial t$ are given in terms of Lagrangian coordinates, yielding successively to:

$$\frac{\partial v_\theta}{\partial t} = \frac{\partial r\dot{\theta}}{\partial t} = \frac{\partial r\dot{\theta}}{\partial a}\frac{\partial a}{\partial t} + \frac{\partial r\dot{\theta}}{\partial \tau},\ \dot{\theta} = \dot{\theta}(a,\tau) = \frac{\partial \theta}{\partial \tau},$$

$$\frac{\partial v_r}{\partial t} = \frac{\partial \dot{r}}{\partial t} = \frac{\partial \dot{r}}{\partial a}\frac{\partial a}{\partial t} + \frac{\partial \dot{r}}{\partial \tau},\ \dot{r} = \dot{r}(a,\tau) = \frac{\partial r}{\partial \tau},$$

and:

$$\frac{\partial v_\theta}{\partial t} = \frac{r}{\partial r/\partial a}\left(\frac{\partial \dot{\theta}}{\partial \tau}\frac{\partial r}{\partial a} - \frac{\partial \dot{\theta}}{\partial a}\frac{\partial r}{\partial \tau}\right),$$

$$\frac{\partial v_r}{\partial t} = \frac{1}{\partial r/\partial a}\left(\frac{\partial \dot{r}}{\partial \tau}\frac{\partial r}{\partial a} - \frac{\partial \dot{r}}{\partial a}\frac{\partial r}{\partial \tau}\right).$$

The right-hand members are zero for a steady velocity field, leading to the double condition:

$$\frac{\partial \dot{\theta}/\partial \tau}{\partial \dot{\theta}/\partial a} = \frac{\partial r/\partial \tau}{\partial r/\partial a} = b(a), \qquad [3]$$

where $b(a)$ is a function of the initial radial coordinate giving the radial velocity versus a at $\tau = 0$.

Condition [3] must be verified for any rotationally invariant steady flow. It should be noted that r depends only on a and τ, but the polar angle θ depends on the initial polar angle α as well:

$$\theta = \theta(a,\alpha,\tau),\ \alpha = \theta(a,\alpha,0),$$

whereas $\dot{\theta}$ depends only on a and τ. This means:

$$\theta = \alpha + \theta_0(a,\tau),\ \theta_0(a,0) = 0. \qquad [4]$$

Condition [4] is always satisfied for any rotationally invariant flow, regardless of whether it is steady or not.

The particle concentration ρ_p, defined as the mass of condensed phase contained in the unit volume of the mixture, for a rotationally invariant flow depends only on r and t in Eulerian variables and therefore on a and τ in Lagrangian variables. In Eulerian variables, it verifies the equation:

$$\frac{\partial(r\rho_p)}{\partial t}+\frac{(v_{pr}r\rho_p)}{\partial r}=0, \qquad [5]$$

and in Lagrangian variables:

$$\frac{\partial}{\partial\tau}\left(r\rho_p\frac{\partial r}{\partial a}\right)=0,$$

yielding:

$$\rho_p(a,\tau)=\frac{a\rho_p(a,0)}{r(\partial r/\partial a)}. \qquad [6]$$

It should be noted that a steady velocity field, which therefore verifies double equation if it is rotationally invariant, can give an unsteady density distribution, as demonstrated by the following examples.

2. VORTEX WITH CONCENTRATED VORTICITY

The fluid flow is irrotational outside a singularity which is located at one point if the flow is two-dimensional. The circulation Γ is constant on any closed curve surrounding the center of the vortex. The gas velocity vector components in polar coordinates are therefore:

$$v_{gr}=0,\ v_{g\theta}=\Gamma/2\pi r. \qquad [7]$$

This velocity field verifies the momentum and continuum equations for constant density fluid flows (ρ_G is constant).

From a practical standpoint, this type of vortex is the idealization of the flow created by an infinitely thin rod rotating at high velocity around itself in a fluid at rest at infinity. If the rod is removed, the vortex becomes free and, assuming that its center remains steady, the vortex is damped by viscosity according to:

$$v_{gr}=0,\ v_{g\theta}=\frac{\Gamma}{2\pi r}\left[1-\exp\left(-\frac{r^2}{4vt}\right)\right]$$

where $v=\mu/\rho g$ is the kinematic viscosity. The vorticity is no longer concentrated but extends to a viscous core whose radius increases as $\sqrt{vt}$. Similarly, certain steady flows have a viscous core. An usual approximation assumes that the motion is that of an undistorted solid rotating uniformly within a circle of radius R connected on the outside to the irrotational vortex. This last model leads to the Rankine vortex. The vortex whose vorticity is concentrated at a point corresponds to the Rankine vortex for which $R\to 0$.

Another structure, for which the velocity field satisfies the Navier–Stokes equations, is the Burgers vortex (Burgers, 1948). It defines a steady three-dimensional flow as follows:

$$v_{gr}=-\sigma r,\ v_{g\theta}=\frac{\Gamma}{2\pi r}\left[1-\exp\left(-\frac{r^2}{2\delta^2}\right)\right],\ v_{gz}=2\sigma z,$$

where σ denotes the strain and $\delta=\sqrt{v/\sigma}$ is the core size. One can see that for $r\gg\delta$, the angular component of the velocity tends to the irrotational angular component ([7]) and that for r becomes $<\delta$, the angular velocity is constant.

2.1. *Analysis of particle motion*

The reference time t_{ref} is the relaxation time τ_v involved in the particle momentum equation. It is the relaxation time necessary for the particle to reach the velocity of the constant velocity fluid. The given circulation Γ is then used to define reference length and velocity such that:

$$l_{\text{ref}}=r_v=\sqrt{\Gamma\tau_v/2\pi},\ v_{\text{ref}}=\sqrt{\Gamma/2\pi\tau_v} \qquad [8]$$

Table 1.

Case	$m+p$	Case	q	Results along θ	Case		Results along r	Results in vector format	Particle movement
I	>0	1	$>m+p$	$\frac{1}{r}\frac{\mathrm{d}}{\mathrm{d}t}(r^2\dot{\theta})=0$	a	$m+q=p$	$\ddot{r}-r\dot{\theta}^2=0, \ddot{r}=\frac{a^4\beta^2}{r^3}$	$\frac{d_p\mathbf{v}_p}{\mathrm{d}t}=0$	Uniform movement in a straight line
				$r^2\dot{\theta}=a^2\beta$	b	$m+q>p$	$\ddot{r}=0$		$r=a+bt, \theta=\alpha-\frac{a^2\beta}{b(a+bt)}+\frac{a\beta}{b}$
		2	$=m+p$	$\frac{1}{r}\frac{\mathrm{d}}{\mathrm{d}t}(r^2\dot{\theta})=0$	a	$q>p$	$\ddot{r}=0$		$r=a+bt, \theta=\alpha+\frac{1}{b^2}\log\frac{a+bt}{a}-\frac{(ab\beta-1)t}{b(a+bt)}$
				$r^2\dot{\theta}=a^2\beta+t$	b	$q=p$	$\ddot{r}-r\dot{\theta}^2=0, \ddot{r}=\frac{(a^2\beta+t)^2}{r^3}$	$\frac{d_p\mathbf{v}_p}{\mathrm{d}t}=\mathbf{v}_g$	Particle acceleration equal to the gas velocity
II	$=0$	1	>0	$\frac{1}{r}\frac{\mathrm{d}}{\mathrm{d}t}(r^2\dot{\theta})=0$	a	$2p=q$	$\ddot{r}-r\dot{\theta}^2=0, \ddot{r}=\frac{a^4\beta^2}{r^3}$	$\frac{d_p\mathbf{v}_p}{\mathrm{d}t}=0$	Uniform movement in a straight line
				$r^2\dot{\theta}=a^2\beta$	b	$2p<q$	$\ddot{r}=0$		Same as I1b
		2	$=0$	$\frac{1}{r}\frac{\mathrm{d}}{\mathrm{d}t}(r^2\dot{\theta})=\frac{1}{r}-r\dot{\theta}$	a	$p<0$	$\ddot{r}=-\dot{r}$		$r=a+b(1-e^{-t}), \theta=\theta(t)$
				$r^2\dot{\theta}=1+(a^2\beta-1)e^{-t}$	b	$p=0$	$\ddot{r}-r\dot{\theta}^2=-\dot{r}$	$\frac{d_p\mathbf{v}_p}{\mathrm{d}t}=\mathbf{v}_g-\mathbf{v}_p$	General undegenerated case
		3	<0	$0=\frac{1}{r}-r\dot{\theta}$	a	$4p=q$	$-r\dot{\theta}^2=-\dot{r}, \dot{r}=\frac{1}{r^3}$		$r^4=4t+a^4, \theta=\alpha-\frac{a^2}{2}+\sqrt{t+\frac{a^4}{4}}$
				$r^2\dot{\theta}=1$	b	$4p<q$	$0=-\dot{r}$	$0=\mathbf{v}_g-\mathbf{v}_p$	The particle follows the gas
III	<0	1	>0	$\frac{1}{r}\frac{\mathrm{d}}{\mathrm{d}t}(r^2\dot{\theta})=0$	a	$m=p$	$\ddot{r}-r\dot{\theta}^2=0, \ddot{r}=\frac{a^4\beta^2}{r^3}$	$\frac{d_p\mathbf{v}_p}{\mathrm{d}t}=0$	Uniform movement in a straight line
				$r^2\dot{\theta}=a^2\beta$	b	$m>p$	$\ddot{r}=0$		Same as I1b
		2	$=0$	$\frac{1}{r}\frac{\mathrm{d}}{\mathrm{d}t}(r^2\dot{\theta})=-r\dot{\theta}$	a	$m=p$	$\ddot{r}-r\dot{\theta}^2=-\dot{r}, \ddot{r}+\dot{r}=\frac{a^4\beta_e^{2-2t}}{r^3}$	$\frac{d_p\mathbf{v}_p}{\mathrm{d}t}=\mathbf{v}_p$	Damped movement in a straight line
				$r^2\dot{\theta}=a^2\beta e^{-t}$	b	$m>p$	$\ddot{r}=-\dot{r}$		$r=a+b(1-e^{-t}), \theta=\theta(t)$
		3	<0	$0=-r\dot{\theta}$ $\dot{\theta}=0$			$0=-\dot{r}$	$0=-\mathbf{v}_p$	Unmoving

The chosen reference length r_v is the distance to the center of the vortex at which the fluid travels $1/2\pi$ circumference in a time τ_v and the corresponding angular velocity component is then the reference velocity. Reference time and length decrease with decreasing particle density and radius and with increasing viscosity. Reference length decreases with Γ. When made dimensionless in this way, [1], considering [7], becomes:

$$\frac{d_p \mathbf{v}_p}{\mathrm{d}t} = \frac{1}{r}\mathbf{e}_\theta - \mathbf{v}_p. \qquad [9]$$

For simplicity the same symbols have been kept in [9] and in the following equations for dimensionless parameters.

If θ and r are the particle's angular and radial dimensionless coordinates, we then have along θ and r respectively:

$$\frac{1}{r}\frac{\mathrm{d}(r^2\dot{\theta})}{\mathrm{d}t} = \frac{1}{r} - r\dot{\theta}, \qquad [10]$$

$$\ddot{r} = r\dot{\theta}^2 = -\dot{r}, \qquad [11]$$

where $\dot{r},\ddot{r},\dot{\theta}$ are the time derivatives of the particle position variables. The solution of this system of equations depends on four integration constants, which are the values at time $t = 0$:

$$r(0) = a,\ \theta(0) = \alpha,\ \dot{r}(0) = b,\ \dot{\theta}(0) = \beta \qquad [12]$$

A first integration of [10] yields (Soo, 1990):

$$r^2\dot{\theta} = 1 + (a^2\beta - 1)e^{-t} \qquad [13]$$

Substituting this in [11] yields:

$$\ddot{r} + \dot{r} = \frac{[1 + (a^2\beta - 1)e^{-t}]^2}{r^3}. \qquad [14]$$

Solving [13] and [14] with [12] gives the particle trajectories and the variation of the particle position as a function of time.

No use has been made of a hydrodynamic characteristic length that would be independent of the vortex and particle characteristics. If such a hydrodynamic length L was introduced, no characteristic dimensionless number would appear here and a characteristic time: $T = 2\pi\ L^2/\Gamma$ could be defined as the time for the fluid to travel $1/2\pi$ circumference of the circle of radius L. A Stokes number S_t could then be introduced by comparison between the two times τ_v and T:

$$\mathrm{S_t} = \tau_v/T = r_v^2/L^2.$$

The advantage of this last formulation is that the variations of τ_v and r_v with the particle and vortex parameters are directly determined by the Stokes number. However the advantage of the formulation chosen lies in the simplicity of the equations obtained. The usual discussion concerning the value of S_t is replaced here by a discussion about the orders of the dimensionless variables r and t (small values of S_t mean that times higher than τ_v and radius larger than r_v are considered. Inversely, high values of S_t correspond to small time and distance from the vortex center).

As it can be seen later, the immediate consequence is that if $r \gg l_\mathrm{ref}$, then the particle will respond quickly to the changing flow direction and the inertial drift radially outwards will be weaker. If $r \ll l_\mathrm{ref}$ the inertia has a strong impact on the particle trajectory. The scaling expansion is effective because the flow has no defined length scale and is singular at the origin. A variety of renormalization constraints may then be adopted.

To display the asymptotic behavior of the system, a multiple scale method is used, setting:

$$r = \varepsilon^p \bar{r},\ t = \varepsilon^q \bar{t},\ v_{pr} = \varepsilon^n \bar{v}_{pr},\ v_{p\theta} = \varepsilon^m \bar{v}_{p\theta}, \qquad [15]$$

where the number ε is small compared with unity, allowing small, large or 0(1) values for each

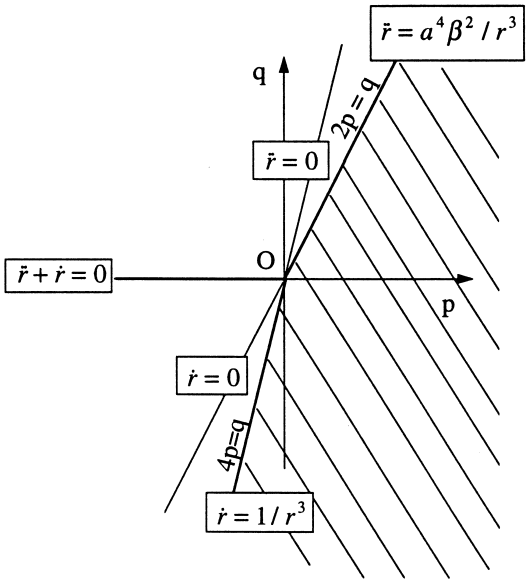

Figure 1. Position in plane (p,q) (orders of magnitude: ε^p of the distance to the center of the vortex and ε^q of the time) of the solutions of case II for which $v_{p\theta}$ and $v_{g\theta}$ are assumed to be of the same order of magnitude.

of the above four parameters. The variables $\bar{r}$, $\bar{t}$, $\bar{v}_{pr}$, $\bar{v}_{p\theta}$ are 0(1) by definition. For instance, $p > 0$ means that the distances investigated in the center of the vortex are very small compared with the reference length given in [8].

For each choice of p, q, m, and n, the time and space derivatives like $\mathrm{d}\bar{r}/\mathrm{d}\bar{t}$, $\mathrm{d}\bar{v}_{pr}/\mathrm{d}\bar{t}$ are assumed to be 0(1) for the reduced quantities. In particular, since $v_{pr} = \mathrm{d}r/\mathrm{d}t$, we infer that:

$$n = p - q \qquad [16]$$

The integration constant of [13] and [14] will be:

$$a^2\beta = \varepsilon^{m+p}\bar{a}^2\bar{\beta} \qquad [17]$$

since $a\beta$ is equal to $r\dot{\theta}$, i.e. to $v_{p\theta}$ at time $t = 0$.

Applying the above definitions to the variation of polar angle θ yields to:

$$\theta = \alpha + \varepsilon^l\bar{\theta}, \text{ where } l = m + q - p \qquad [18]$$

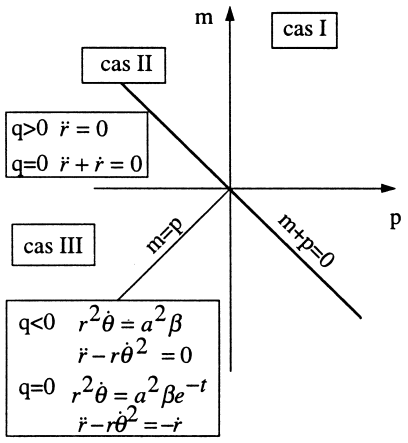

Figure 2. Position in plane (p,m) characterizing the orders of magnitude of r and $v_{p\theta}$ respectively for the different cases, in particular the solutions of case III where $v_{p\theta} \gg v_{g\theta}$.

[13] and [14] which completely describe the particle motion are written:

$$\varepsilon^{m+p}\,\bar{r}^2\,\frac{\mathrm{d}\bar{\theta}}{\mathrm{d}\bar{t}} = 1 + (\varepsilon^{m+p}\bar{a}^2\bar{\beta} - 1)e^{-\varepsilon^q\bar{t}} \qquad [19]$$

$$\varepsilon^{4p-2q}\,\frac{\mathrm{d}^2\bar{r}}{\mathrm{d}\bar{t}^2} + \varepsilon^{4p-q}\,\frac{\mathrm{d}\bar{r}}{\mathrm{d}\bar{t}} = \frac{1}{\bar{r}^3}\left[1 + (\varepsilon^{m+p}\bar{a}^2\bar{\beta} - 1)e^{-\varepsilon^q\bar{t}}\right]^2 \qquad [20]$$

Depending on the values chosen for m, p and q (from which n and l are deduced according to [16] and [18]), certain terms of equations [17] and [18] may vanish, which then allows an analytic solution.

Table 1 shows all the possible solutions to this problem. It can be seen that certain approximations could have been made directly in [9], for which the five degenerate cases as well the undegenerate case (II2b) can be seen in the table. The other approximations correspond to degenerate cases specific to the polar coordinates associated with the characteristics of the gas vortex selected. Five other degenerate cases appear. The solutions for these cases may be determined analytically.

It may be worthwhile to show the solutions of case II in the plane (p,q), since ε^p and ε^q represent the orders of magnitude of r and t respectively in the sense where, for instance, $p > 0$ means $r \ll 1$, $p = 0$ gives $r = 0(1)$ and $p < 0$ corresponds to $r \gg 1$ (figure 1).

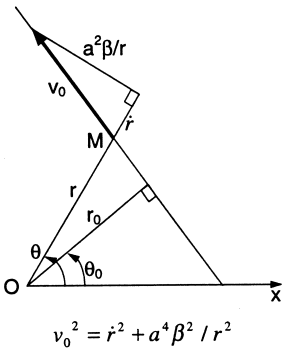

a - Case of uniform motion in a straight line
The particle does not see the gas

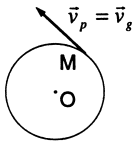

b - Case of circular motion
The particle follows the gas, its inertia is negligible

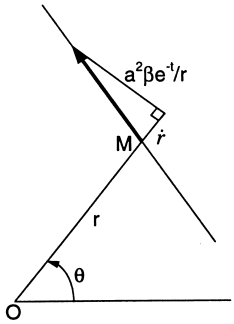

c - Case of damped motion in a straight line
The particle is slowed down by the gas whose motion it does not see

d - Case at rest

Figure 3. Representation in the physical plan for three elementary movements.

Table 2. Solutions of case I $v_{p\theta} \ll v_{g\theta}$

I1a (see figure 3a)—Uniform motion in a straight line	$v_{pr} = v_0\sqrt{1-\frac{r_0^2}{r^2}},\ v_0^2 = b^2 + a^2\beta^2,\ r_0^2 = \frac{a^4\beta^2}{b^2+a^2\beta^2}$ $v_{p\theta} = \frac{a^2\beta}{r}$
I1b	$v_{pr} = b,\ r = a + bt,\ \theta = \alpha + \frac{a\beta}{b} - \frac{a^2\beta}{b(a+bt)}$ $v_{p\theta} = \frac{a^2\beta}{r},\ \theta = \alpha + \frac{a\beta}{b}\left(1-\frac{a}{r}\right)$
I2a	$v_{pr} = b,\ r = a + bt,\ \theta = \alpha + \frac{1}{b^2}\log\frac{r}{a} - \frac{1}{b}\left(a\beta - \frac{1}{b}\right)\left(1-\frac{a}{r}\right)$ $v_{p\theta} = \frac{1}{b} + \frac{a(ab\beta-1)}{br}$
I2b	A Taylor series expansion is carried out around $t = 0$ giving in the third order $r = a + bt + \frac{a\beta^2}{2}t^2,\ \theta = \alpha + \beta t + (1-2ab\beta)$ $v_{pr} = \sqrt{b^2a\beta^2(r-a)},\ v_{p\theta} = b\left(\frac{\beta}{b} - \frac{1-2ab\beta}{a^3\beta^2}\right)r + \frac{1-2ab\beta}{a^2\beta}r\sqrt{\frac{b^2}{a^2\beta} - 2 + \frac{2r}{a}}$

The positions of the solutions of case III, for which it is assumed $v_{p\theta} \gg v_{g\theta}$, are shown in plane (p,m) (figure 2); ε^p represents the order of magnitude of the radial coordinate and ε^m that of velocity $v_{p\theta}$.

The trajectories are easy to obtain in the physical plane for cases (I1a), (II1a) and (III1a) corresponding to a uniform motion in a straight line (figure 3a), for case (II3b) where the particle follows the gas (figure 3b), for case (III2a) of damped rectilinear motion (figure 3c) and case (III3) of the unmoving particle (figure 3d). In figure 3a, the position of the trajectory is defined by r_0 and θ_0. The particle velocity is v_0.

The use of multiple scales expansions allows one to distinguish between the ranges $t \ll 1$, $t \sim 1$, or $t \gg 1$ and these correspond to case II. A common approach is to apply matching between the expansions. For $t \ll 1$ the initial condition of the particle momentum is important, but for $t \gg 1$ this becomes $r^2\dot{\theta} = 1$. The exponential coefficient means that $t \geq 3$ suffices for $t \gg 1$. The conditions I1a, II1a, III1a are for a particle with such strong inertia that, whatever

Table 3. Solutions of case II $v_{p\theta} = 0(v_{g\theta})$

II1a uniform motion in a straight line (same as I1a)	
II1b	Same as I1b
II2a	$r = a + b(1-e^{-t}),\ \theta = \alpha + \frac{1}{b}\left(a\beta - \frac{1}{a+b}\right)\left[1 - \frac{a}{a+b(1-e^{-t})}\right] + \frac{t + \frac{\log[a+b(1-e^{-t})]}{a}}{(a+b)^2}$ $v_r = a + b - r,\ v_\theta = \frac{1-a^2\beta}{b} + \left[1 + (a^2\beta - 1)\left(\frac{a}{b}+1\right)\right]\frac{1}{r}$
II2b	Numerical solution, undegenerated case
II3a	$v_r = \frac{1}{r^3},\ v_\theta = \frac{1}{r},\ \theta = \alpha - \frac{a^2}{2} + \frac{r^2}{2}$
II3b	Uniform rotation $r = a,\ v_r = o,\ v_\theta = \frac{1}{a}$

Table 4. Solutions of case III $v_{p\theta} \gg v_{g\theta}$

III1a	Uniform motion in a straight line (same as I1a)
III1b	Same as I1b
III2a	(see figure 3c)-Damped motion in a straight line
III2b	Same as II2a taking $a^2\beta \to \infty$
	$r = a + b(1 - e^{-t}),\ \theta = \alpha + \dfrac{a\beta}{b}\left[1 - \dfrac{a}{a + b(1 - e^{-t})}\right] + \dfrac{t + \dfrac{\log\,[a + b(1 - e^{-t})]}{a}}{(a + b)^2}$
	$v_r = a + b - r,\ v_\theta = -\dfrac{a^2\beta}{b} + \left[1 + a^2\beta\left(\dfrac{a}{b} + 1\right)\right]\dfrac{1}{r}$
III3	$r = a,\ \theta = \alpha$

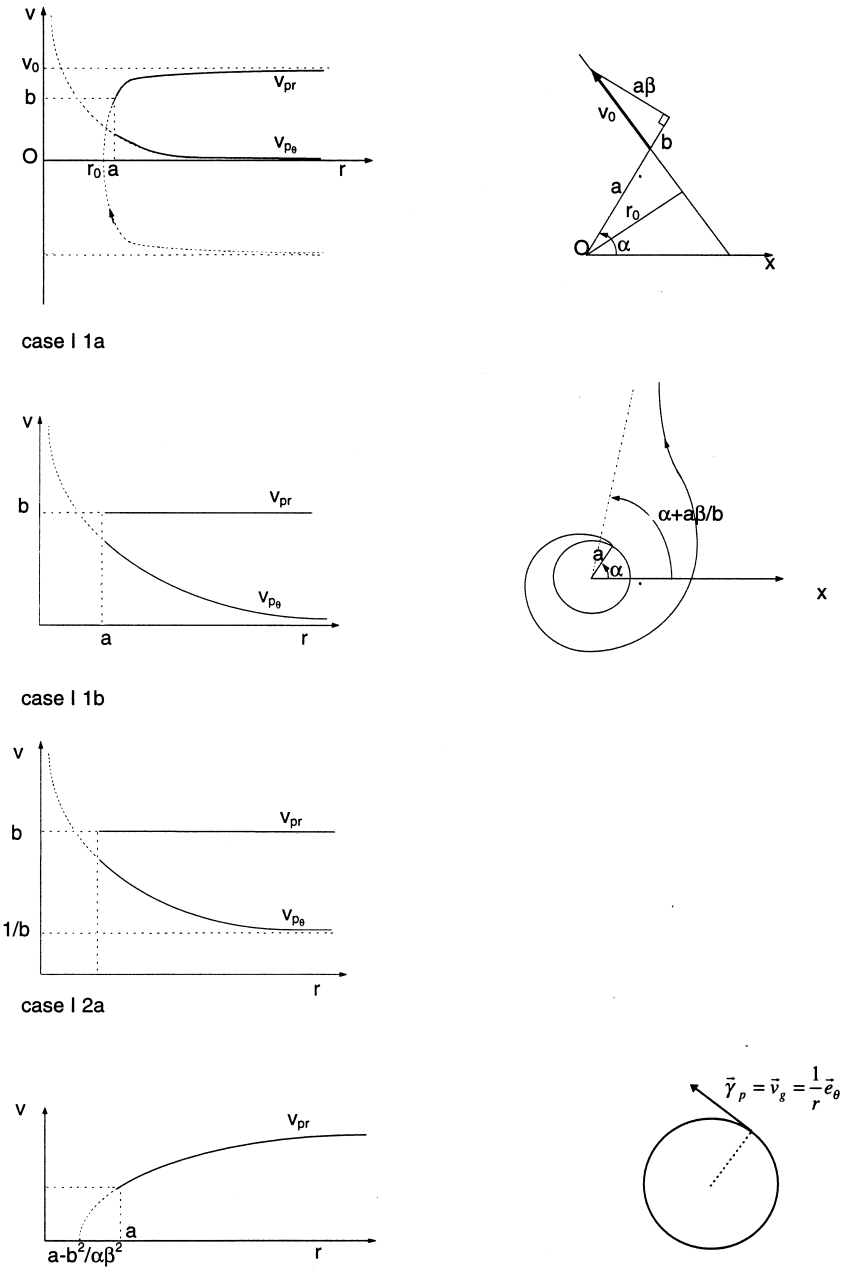

Figure 4. Case I ($v_{p\theta} \gg v_{g\theta}$). Path representations in plan (r,v) and in the physical plan.

its initial location relative to the point vortex, the particle continues unaffected with constant linear momentum. This can only persist for $t < 1$ since eventually the viscous drag forces will bring the particle to rest. The condition III2a is more general and physically accounts for the previous three conditions also. Here the influence of the vortex is negligible and the particle continues on a straight line before coming to rest.

The example II3b would arise for a particle exhibiting relatively little inertia but trapped by the vortex and spiraling slowly from the completely circular path of a fluid element. In this context $r \gg 1$ so that $1/r$ is a small parameter.

The solutions are developed for each case in tables 2–4.

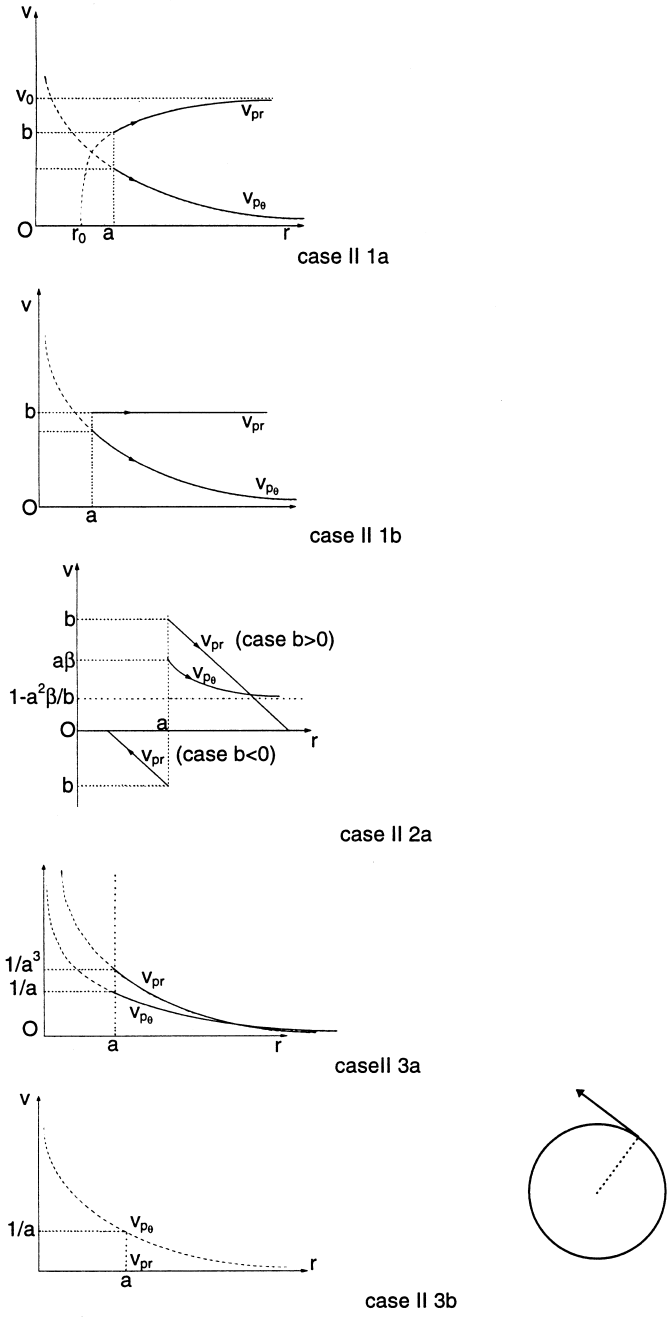

Figure 5. Case II [$v_{p\theta} = 0(v_{g\theta})$]. Path representations in plane (r,v) and in the physical plane.

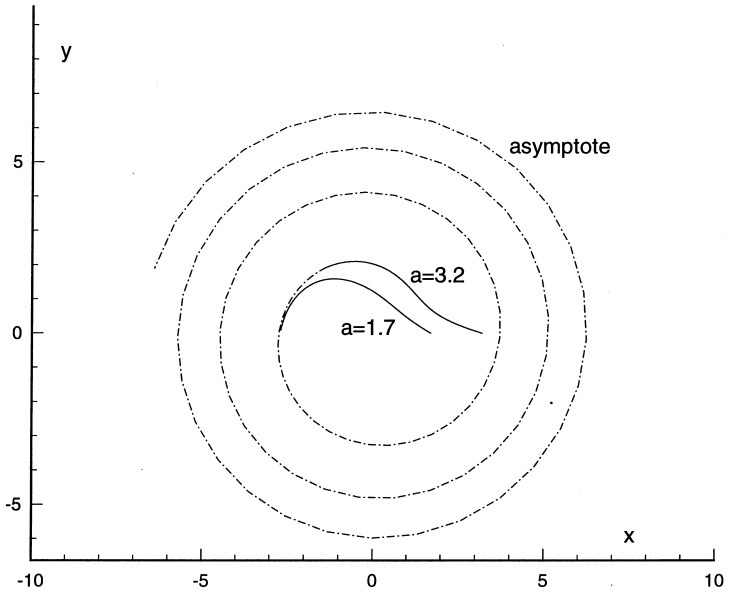

Figure 6. Example of numerically computed path ($a^2\beta = 2$, $b = -2$).

Finally, the curves corresponding to the different solutions are given in the plane (*r*, *velocity*) and, where possible, in the physical plane, figures 4 and 5.

Figure 6 is an example of numerical result in the undegenerate case. It shows two trajectories which, after moving away from each other, tend to move together and converge on a spiral which is a common asymptote. The turns tend to become closer as time goes by, which is easily explained by the asymptotic behavior II3a.

Before examining a particle continuum, the physical assumptions should be recalled. For an individual particle in the vortex:

—the particle size must be small compared with the distance to the center of the vortex;
—the Reynolds number of the particle must be sufficiently small to verify Stokes's theory;
—the conditions must be satisfied for the other drag terms to be negligible compared with the Stokes terms. In particular, this means that the gas density must be very small compared with the particle density and the accelerations must not be too large (see Appendix A).

For the continuum (two-phase medium), the assumptions regarding dilute suspensions are assumed to be verified. In particular, the volume occupied by the particles must be negligible compared with the volume of gas. This assumption is no longer verified for high particle concentrations, ρ_p. It will be seen that there are cases where the particles tend to collect in certain regions. If the distance between particles becomes too small, the theory of suspensions without interactions between particles is no longer valid and, if this distance becomes very small and in presence of high gradients, even the continuum hypothesis may no longer be valid, in which case shocks may occur.

2.2. *Analysis of the particle continuum motion*

The above analysis naturally leads one to consider the particle continuum forming the suspension in terms of Lagrangian coordinates. In effect, the above equations and results are valid, but the question of continuity arises and discontinuity waves may occur. The description using Eulerian coordinates will then be examined, assuming only one particle size.

The particle continuum verifies [1] which takes form [9] for the gas vortex with concentrated vorticity and yields [10] and [11] in Lagrangian coordinates with:

$$r = r(a,\tau),\ \dot{r} = \frac{\partial r}{\partial \tau},\ a = r(a,0),\ b = \dot{r}(a,0), \qquad [21]$$

$$\theta = \alpha + \theta_0(a,\tau),\ \dot{\theta} = \frac{\partial \theta}{\partial \tau},$$

$$0 = \theta_0(a,0),\ \beta = \dot{\theta}(a,0), \qquad [22]$$

assuming the solutions to be rotationally invariant ([4]). However, considering a continuum also requires specification of the functions:

$$b = b(a) \text{ and } \beta = \beta(a) \qquad [23]$$

The form of these functions determine whether or not the particle flow is a continuum and the steady or unsteady nature of certain solutions.

The example of case I1a (or II1a or III1a) is considered. Each particle moves in a straight line and then:

$$r^2 = r_0^2 + \left(v_0 t + \frac{ab}{v_0}\right)^2,\ v_0^2 = b^2 + a^2\beta^2,\ v_{pr} = v_0\sqrt{1 - \frac{r_0^2}{r^2}},\ r_0^2 = \frac{a^4\beta^2}{b^2 + a^2\beta^2},\ v_{p\theta} = \frac{a^2\beta}{r}. \qquad [24]$$

r_0 and v_0 are defined on figure 7.

If r_0 and v_0 are constant and given the following functions of a for β and b:

$$\beta = \frac{K}{a^2},\ b^2 = K^2\left(\frac{1}{r_0^2} - \frac{1}{a^2}\right), \qquad [25]$$

this yields:

$$v_{pr}^2 = K^2\left(\frac{1}{r_0^2} - \frac{1}{r^2}\right),\ v_{p\theta} = \frac{K}{r},\ r \geqslant a \geqslant r_0, \qquad [26]$$

i.e. a continuous solution for $r \geq r_0$ provided one of the positive or negative roots is taken to provide v_{pr} in [26]. This solution is also steady. The velocity field is deduced with $v_0 > 0$ as shown in figure 7a; there are no particles inside the circle of radius r_0. Cases where $b_0 < 0$, verify-

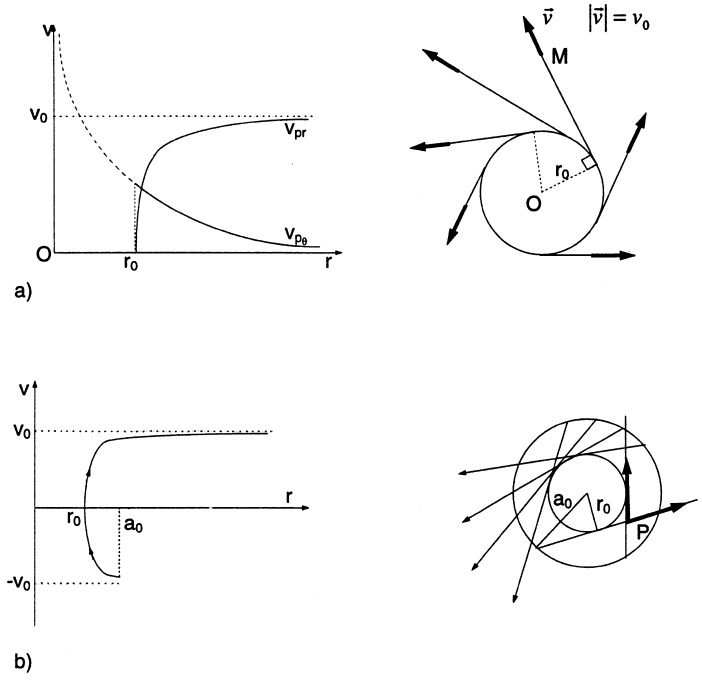

Figure 7. Dispersed phase motions for given values of r_0 and v_0.

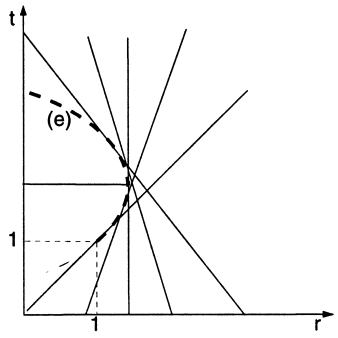

Figure 8. Possible formation of a discontinuity wave.

ing [25], can also be considered with v_0 remaining positive. The particles again follow the same rectilinear paths but first move toward the center O before moving away from it. In a region $r_0 \leq r \leq a_0$, there are two determinations of v_{pr} for any point P; this solution is not to be excluded in the case of a flow with particles, whereas it would lead to the formation of a shock in a conventional fluid (figure 7b). Interactions between particles are certainly present in this case, but are not studied here.

Another choice issued from the same basic equations [24] is given by initial conditions verifying:

$$\beta = K/a^2,\ K = C^{te},\ b = 0. \qquad [27]$$

The solutions obtained are unsteady as shown by their expression in Eulerian coordinates:

$$v_{pr} = \left(\frac{r^2}{2t^2} - \frac{K^2}{r^2} \pm \sqrt{\frac{r^4}{t^4} - \frac{4K^2}{t^2}}\right)^{1/2},\ v_{p\theta} = \frac{K}{4},\ r^2 \geqslant \sqrt{2Kt}. \qquad [28]$$

These solutions are continuous after choosing the positive or negative determination. However, a distribution such that:

$$\beta = 0,\ b^2 - 6b + 5 - 4a = 0$$

leads to multiple solutions whenever $t > 1$, as is shown in figure 8, where the envelope (e) of the trajectories in the plane (r, t) has the equation

$$r = -t^2 + 3t - 1.$$

A possible interpretation of the curve (e) for $t > 1$ could be the formation of a discontinuity. If it is, above $t = 1$, other equations similar to shock equations should therefore be used here.

These examples illustrate the fact that the choice of the functions $b(a)$ and $\beta(a)$ determines the type of solution. In most cases it refers to specific physical situations.

In only three of the cases in table 1, the results do not depend on either $b(a)$ or $\beta(a)$. Among these, case II3a is definitely the most interesting. It reflects the behavior of the suspension for high values of r and t. We have:

$$v_{pr} = 1/r^3,\ v_{p\theta} = 1/r$$

a steady solution approached by any particle motion. Furthermore, the instances of the general case where the product $a^2\beta$ is considered constant and equal to K (as was done above in a special case, see [27]) are also very interesting. [13] and [14] then become:

$$r^2\,\dot{\theta} = 1 + (K - 1)e^{-t}$$

$$\ddot{r} + \dot{r} = [1 + (K-1)e^{-t}]^2/r^3. \qquad [29]$$

For $K = 1$, the particles have the same angular component of velocity as the fluid, but their radial velocity is different due to the centrifugal effect. We have:

$$r\dot{\theta} = 0 \text{ or } v_{pr} = 1/r$$

$$\ddot{r} + \dot{r} = 1/r^3. \qquad [30]$$

One can change variables and take r instead of t for a and b given, i.e. for a given trajectory. Setting $\dot{r} = v(a, b, r)$ yields the following result for the second part of [29]:

$$v\frac{\partial v}{\partial r} + v = \frac{1}{r^3}\left(1 + (K-1)e^{-\int_a^r \frac{dr}{v}}\right). \qquad [31]$$

This equation is considerably simplified when $K = 1$. A view of the trajectories is obtained by calculating $\partial v/\partial r = 1/r^3 v - 1$ and plotting the tangent elements (figure 9). The locus of the maxima is $v = 1/r^3$. Only one system of curves is obtained. On a given trajectory, starting from different initial conditions will lead to the same trajectory, as demonstrated on figure 10 for $b = 0$ and $b = -2$, after computation from [30].

Contrary to the case $K = 1$, the case $K = 2$, for instance, shows after computation that the trajectories obtained with $b = -2$ are different from those plotted with $b = 0$. If a point of the path starting at $b = -2$, $a = 1.7$ is chosen, the result from this new initial point is a new trajectory (figure 11). In addition, the locus of the maxima of v_{pr}, is not unique.

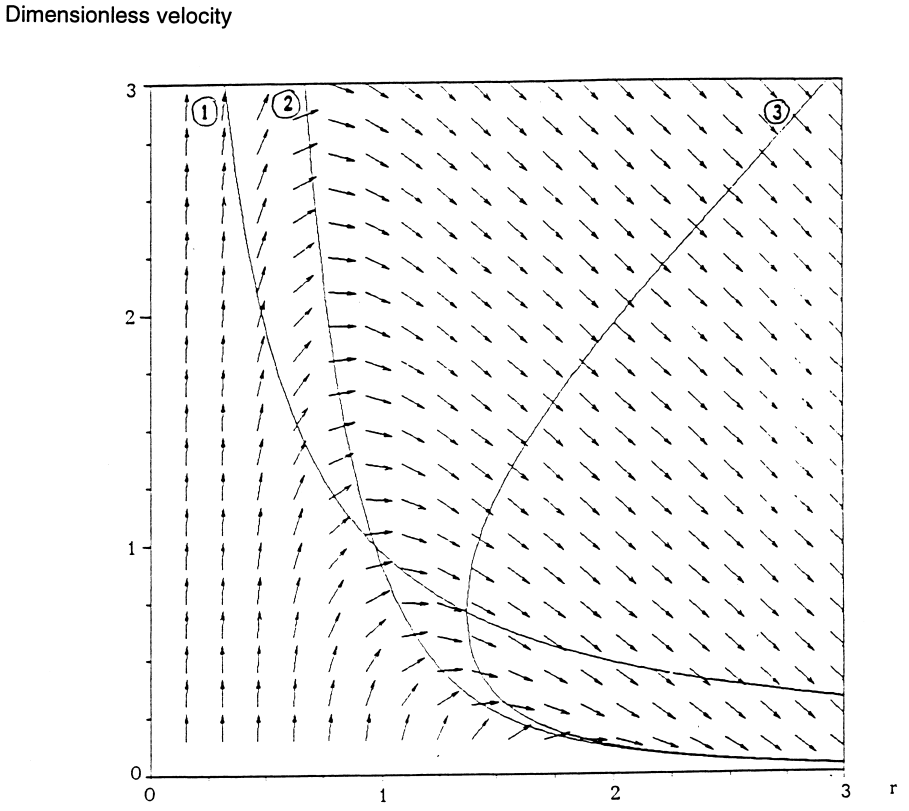

Figure 9. Field of vectors tangent to the curves $v_{pr} = v_{pr}(r)$. Curve 1: $v_{p\theta} = 1/r$; curve 2: $v_{pr} = 1/r^3$; curve 3: locus of points where the product (rv_{pr}) is a maximum (the concentration is minimum).

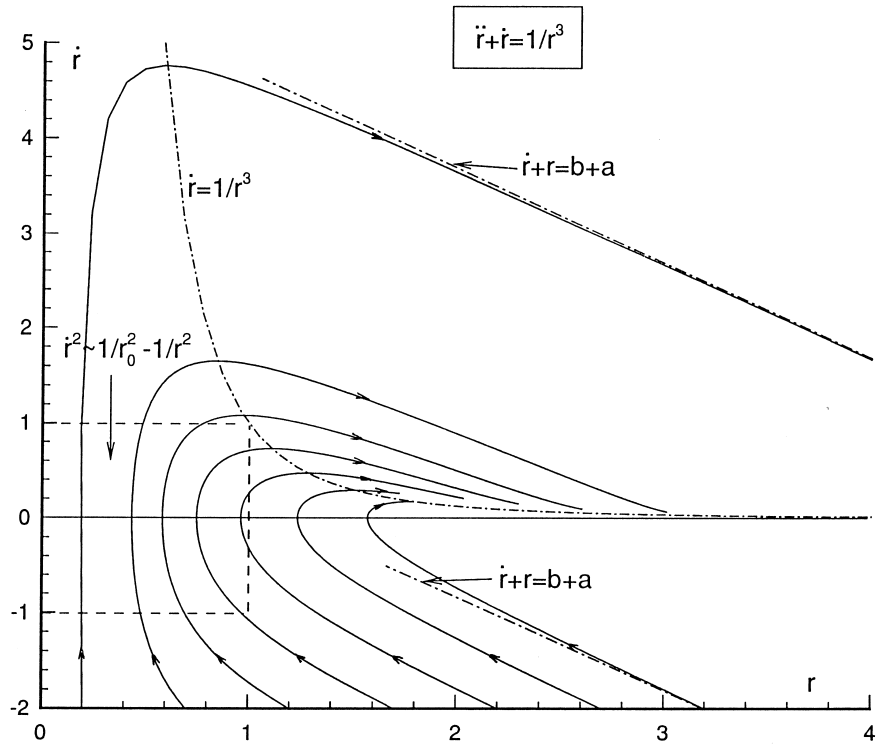

Figure 10. For $a^2\beta = K = 1$, a single system of curves; here $b(a) = -2$, $r_0 = r$ ($\dot{r} = 0$).

Figures 9–11 are very instructive in that the computation is totally coherent with the asymptotic solutions found earlier in case II of table 1. For small values of r and for v_{pr} not too large, behavior II1a is found, giving straight line trajectories in the physical plane. The maximum of v_{pr} corresponds to case II1b. For relatively large values of v_{pr} (positive or negative) and r, the

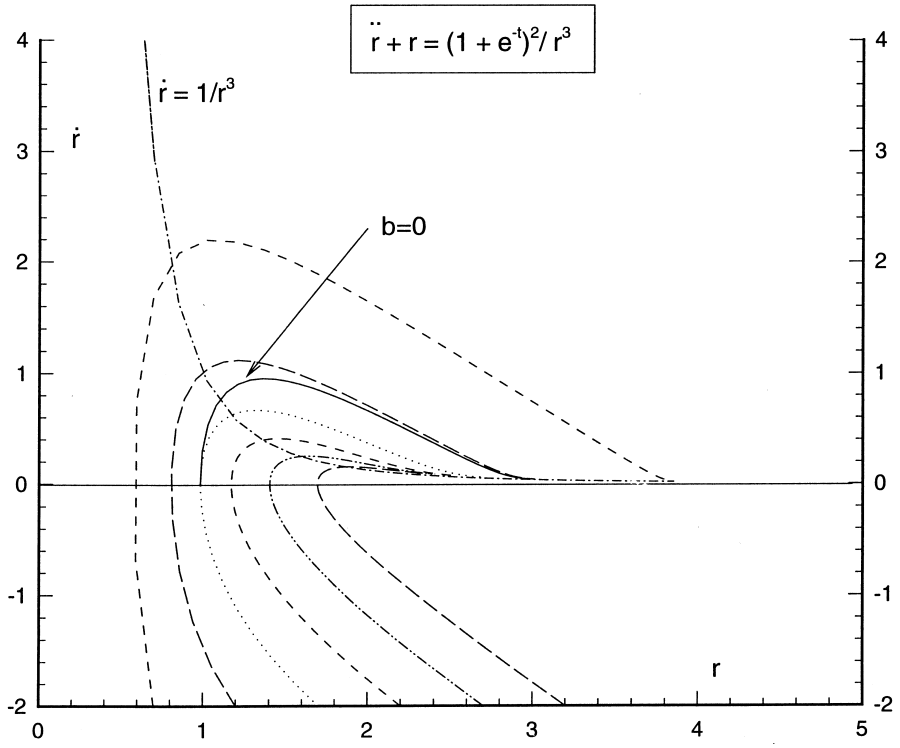

Figure 11. Paths ($a^2\beta = K = 2$, $b(a) = -2$); influence of b on one of the paths.

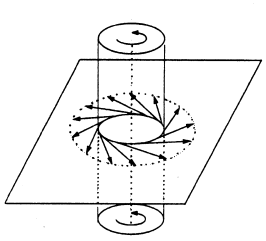

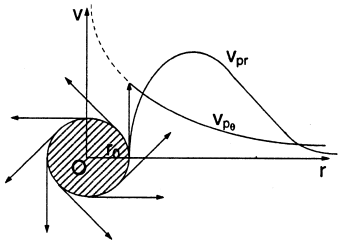

Approximations

II1a *t* and *r* small

$$v_{pr}^2 = \frac{1}{r_0^2} - \frac{1}{r^2}, \quad v_{p\theta} = \frac{1}{r}, \quad r \geq r_0, \quad r = \left(r_0^2 + (\pm \frac{t}{r_0} + \sqrt{a^2 - r_0^2})^2 \right)^{1/2}$$

Particle mass-flow rate: $\dot{m}_p$ constant

$$\rho_p(a,0) = \frac{\dot{m}_p}{2\pi\sqrt{a^2 - r_0^2}}, \quad a \rangle r_0$$

Concentrations:

$$\rho_p = \frac{\dot{m}_p}{2\pi\sqrt{r^2 - r_0^2}}, \quad r \rangle r_0$$

II3a *r* large

$$v_{pr} = \frac{1}{r^3}, \quad v_{p\theta} = \frac{1}{r}, \quad r = \left(4t + a^4\right)^{1/4}$$

$$\rho_p(a,0) = \frac{\dot{m}_p a^2}{2\pi}$$

Concentrations:

$$\rho_p = \frac{\dot{m}_p r^2}{2\pi}$$

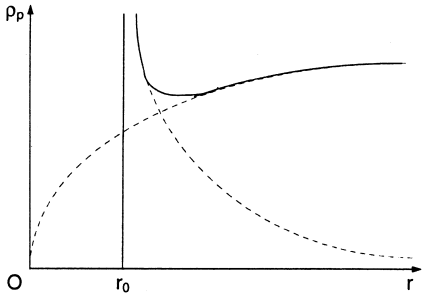

Figure 12. Example of steady flow.

case II2a is characterized by trajectories parallel to the second bisector of plane (r,v). Finally, the curves are very close to the steady path of case II3a for large radii and the particles finish by following the gas motion (case II3b).

Are the general solutions steady for $a^2\beta = K = C^{te}$? Definitely not for $K \neq 1$, since, according to [29], we have:

$$v_{p\theta} = r\dot{\theta} = \frac{1 + (K-1)e^{-t}}{r^3}.$$

However, $K = 1$ yields [30] which shows that $v_{p\theta}$ does not depend on time in Eulerian variables. Is this also true for v_{pr}? The steady or unsteady feature of the flow in Lagrangian variables depends not only on the equations to be solved but also, on functions $b(a)$ and $\beta(a)$.

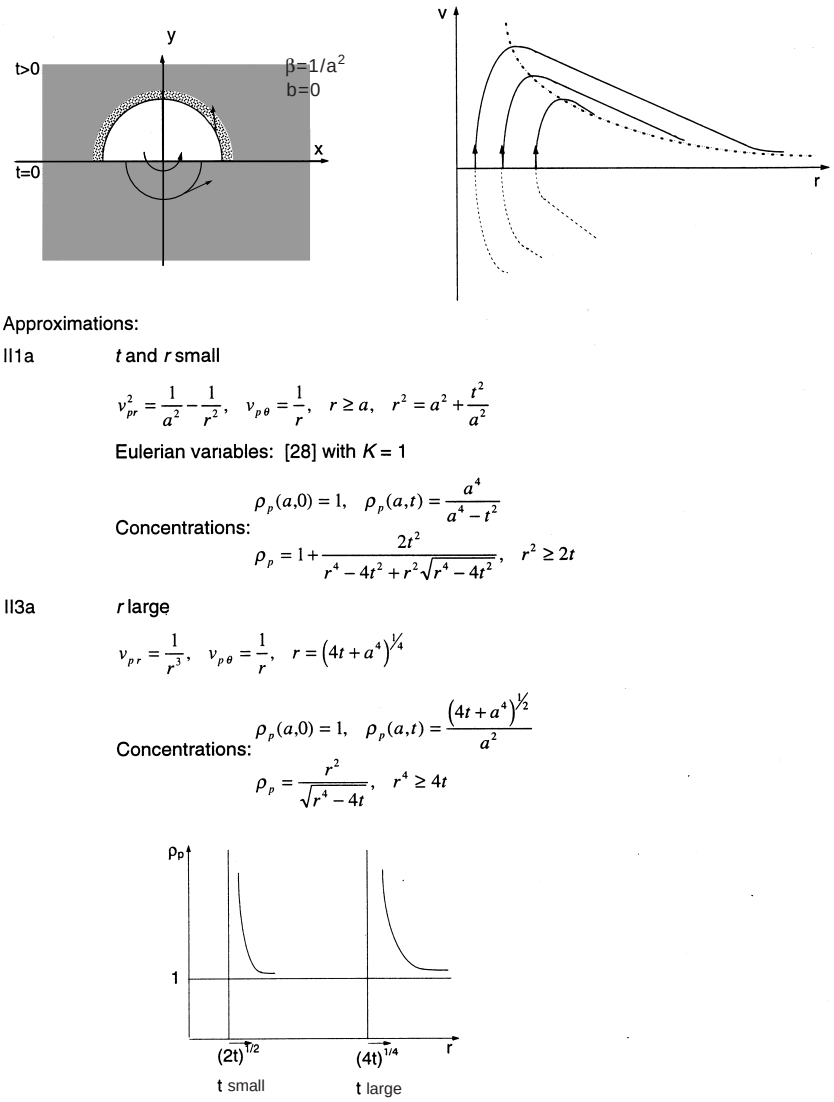

Figure 13. Example of time dependant flow.

Function $\beta(a)$ is set to $1/a^2$ for $K = 1$. The influence of $b(a)$ on the steady character of the flow is then evaluated.

If $b(a)$ is represented by a single curve in figure 10, trajectory $v(r)$ continuously follows this curve. The corresponding physical situation corresponds to the steady two-dimensional fluid flow created by a cylinder of radius r_0 rotating at an angular velocity $1/r_o^2$ and whose porous surface particles are injected at zero relative velocity and constant mass flow rate. The particle flow is then a steady two-dimensional flow and the particle concentration is given by [6] which, taking [3] into account, becomes:

$$\rho(a,t) = \rho(a,0)\frac{ab}{r\dot{r}}.$$

Asymptotic approximations are used to derive the velocities and concentrations analytically (figure 12).

If particle injection is stopped at time $t = t_1$, the particles injected up to that point, $t < t_1$, continue their trajectories without being influenced by the end of injection and the circle with no particles increases with time, following the motion of the last particles injected.

If $b(a)$ is zero for any positive value of a and is always zero for $K = 1$ (i.e. for β(a) equal to $1/a^2$), the trajectories are shown in figure 10. This is the situation of a two-dimensional vortex of saturated vapor. A slight decrease in temperature creates a mist of particles initially carried at the velocity of the gas vortex. The centrifugal force creates a particle hole which is a circle of increasing radius centered at the origin. The particle concentration, zero inside the hole, increases with time at the edges of the hole. This is the case of an unsteady flow (figure 13), which, although very different from the previous one, satisfies the same partial differential equations.

One can also imagine a concrete situation for $K = 0$, that of a suspension at rest for $t < 0$ in which a vortex is suddenly placed. The initial angular velocity β is zero as is the radial velocity b. The particles are then swept away by the flow and subjected to the centrifugal force (figure 14). A hole is created, as in the above case, and the flow is steady.

A steady state solution can only be encountered if the following equation is verified, as easily demonstrated by using [3] and [13]:

$$b(a)\frac{d[a^2\beta(a)]}{da} + a^2\beta(a) = 1. \qquad [32]$$

This means that in the class of solutions $a^2\beta(a) = K = C^{te}$, only $K = 1$ can give steady solutions. Any solution obtained for $K = 1$ such as $\frac{\partial r/\partial \tau}{\partial r/\partial a} = b(a)$ is a steady solution. This condition applied to the second equation of system [30] (or to [14]) yields:

$$\frac{\mathrm{d}b}{\mathrm{d}a} = \frac{1}{a^3 b} - 1, \qquad [33]$$

which is, in fact, verified when $b(a)$ follows a single curve of figure 10.

Let us now discuss the solution in Eulerian coordinates. The above solutions were all obtained using Lagrangian coordinates and the deduction of the asymptotic solutions in Eulerian coordinates can be derived (see [26], [28] and [30] for instance). The advantage of Lagrangian coordinates is that once the initial conditions are given [here $b(a)$ and $\beta(a)$], all that remains to be done is to integrate the equations with respect to time. In Eulerian coordinates, the partial differential equations are with respect to time and space. [10] and [11] are replaced by the system:

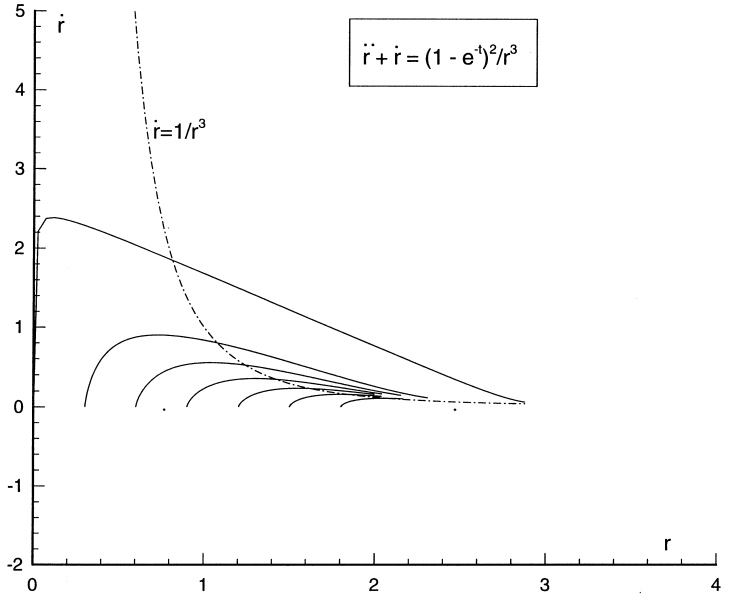

Figure 14. Particles at rest at the initial time, $b(a) = 0$, $\beta(a) = 0$. .

$$\frac{1}{r}\frac{\partial(rv_{p\theta})}{\partial t}+\frac{v_{pr}}{r}\frac{\partial(rv_{p\theta})}{\partial r}=\frac{1}{r}-v_{p\theta},$$

$$\frac{\partial v_{pr}}{\partial t}+v_{pr}\frac{\partial v_{pr}}{\partial r}-\frac{v_{p\theta}^2}{r}=-v_{pr}. \qquad [34]$$

The steady velocity fields have been studied. The above system becomes (Dodemand and Prud'homme, 1991; Dodemand, 1994)

$$v_{pr}\frac{\mathrm{d}v_{p\theta}}{\mathrm{d}r}+\frac{v_{pr}v_{p\theta}}{r}=\frac{1}{r}-v_{p\theta},$$

$$v_{pr}\frac{\mathrm{d}v_{pr}}{\mathrm{d}r}-\frac{v_{p\theta}^2}{r}=-v_{pr}. \qquad [35]$$

As was seen above, such steady velocity fields do exist. Setting, as in [15] except for time:

$$r=\varepsilon^{p}\,\bar{r},\ v_{pr}=\varepsilon^{n}\bar{v}_{pr},\ v_{p\theta}=\varepsilon^{m}\bar{v}_{p\theta}$$

yields:

$$\bar{v}_{pr}\frac{\mathrm{d}\bar{v}_{p\theta}}{\mathrm{d}\bar{r}}+\frac{\bar{v}_{pr}\bar{v}_{p\theta}}{\bar{r}}=\varepsilon^{-(m+n)}\frac{1}{\bar{r}}-\varepsilon^{(p-n)}\bar{v}_{p\theta}$$

$$\bar{v}_{pr}\frac{\mathrm{d}\bar{v}_{pr}}{\mathrm{d}\bar{r}}-\varepsilon^{2(m-n)}\frac{\bar{v}_{p\theta}^2}{\bar{r}}=-\varepsilon^{(p-n)}\bar{v}_{pr}. \qquad [37]$$

Arranging the equations in a table according to the values of $p-n$, $m-n$ and $m+n$ gives a set of results corresponding to those of table 1 taking [16] into account, expressed in r, v_{pr}, $v_{p\theta}$, $\mathrm{d}v_{pr}/\mathrm{d}r$ and $\mathrm{d}v_{p\theta}/\mathrm{d}r$, except for the unsteady terms. Furthermore, cases I1 and III1 no longer appear.

Without making any approximations, it can be seen that if $rv_{p\theta}=1$, we have:

$$v_{pr}\frac{\mathrm{d}v_{pr}}{\mathrm{d}r}+v_{pr}=\frac{1}{r^3}. \qquad [38]$$

The solutions of this equation give the system of curves of figure 10. Each of the curves considered corresponds to a steady flow of the particle continuum. This, in fact, corresponds to what can be found using Lagrangian coordinates and to the concrete case of particle injection from a circle rotating at the velocity of the fluid.

3. RANKINE VORTEX

The Rankine vortex includes a flow inside a circle with radius R where the fluid has a uniform angular velocity Ω. Outside this core, the motion is that of an irrotational vortex with circulation Γ. The velocity connection condition at $r=R$ leads to a relationship between Ω, Γ and R.

This connection gives an angular velocity profile $v_{g\theta}(r)$ (figure 15). Certain authors use a modified Rankine vortex by introducing a function which approaches Ωr for small values of r and $\Gamma/2\pi$ for large values of r to obtain a better velocity profile. The maximum is then continuous instead of exhibiting a velocity peak for $r=R$. To summarize, two cases can be proposed:

The Rankine vortex defined by:

$$r\leq R,\ v_{g\theta}=\Omega r,\ v_{gr}=0,$$

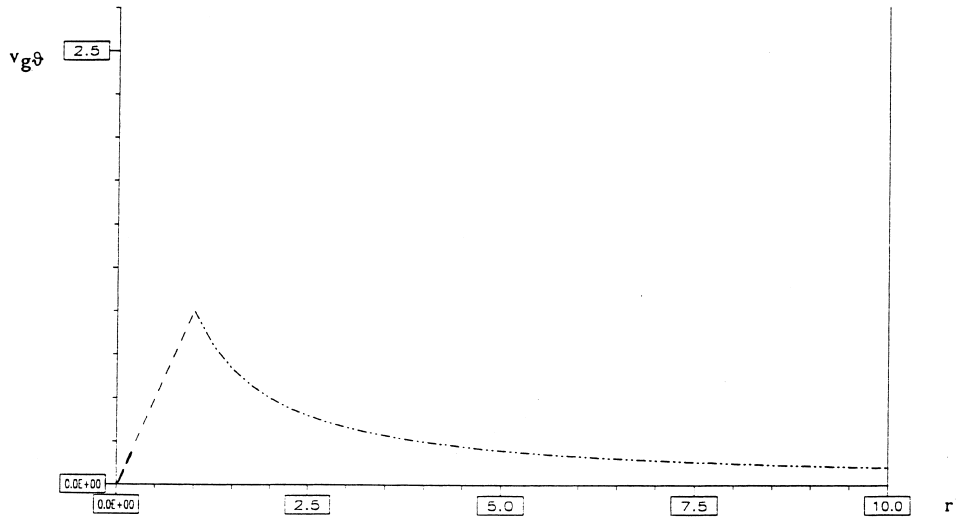

Figure 15. Fluid tangential velocity versus radius.

$$r \geqslant R,\ v_{g\theta} = \Gamma/2\pi r,\ v_{gr} = 0,\ \Omega R = \Gamma/2\pi r. \qquad [39]$$

The modified Rankine vortex defined by:

$$v_{g\theta} = \Omega \frac{R^2 r}{r^2 + R^2},\ v_{gr} = 0. \qquad [40]$$

Introducing the new reference quantities:

$$t_{\text{ref}} = \tau_v,\ l_{\text{ref}} = L,\ v_{\text{ref}} = L/\tau_v. \qquad [41]$$

[1] governing particle motion is written;

$$\frac{d_p \mathbf{v}_p}{\mathrm{d}t} = \varpi r \mathbf{e}_\theta - \mathbf{v}_p,\ \varpi = \Omega\tau_v,\ r \leqslant R. \qquad [42]$$

The dimensionless number ϖ is the ratio of the particle viscous relaxation time to the mechanical fluid angular rotation time. Referring the characteristic radius r_v of the irrotational vortex present for $r \geq R$ ([8]) to radius R yields:

$$r_v/R = \sqrt{\varpi}. \qquad [43]$$

In polar coordinates, [42] becomes:

$$\frac{1}{r}\frac{\mathrm{d}(r^2\dot{\theta})}{\mathrm{d}t} = \varpi r - r\dot{\theta},\ r \leq R, \qquad [44]$$

$$\ddot{r} - r\dot{\theta}^2 = -\dot{r}. \qquad [45]$$

This system is solved numerically, but an asymptotic analysis can be performed as above by using the multiple scales method ([15]). Matching with the irrotational vortex should be carried out on the limit radius $r = R$. [44] and [45] become:

$$\varepsilon^{-q}\frac{\mathrm{d}(\bar{r}^2\dot{\bar{\theta}})}{\mathrm{d}\bar{t}} + \bar{r}^2\dot{\bar{\theta}} = \bar{\varpi}\varepsilon^{2s+p-m}\bar{r}^2,\ \varpi = \varepsilon^{2s}\bar{\varpi}, \qquad [46]$$

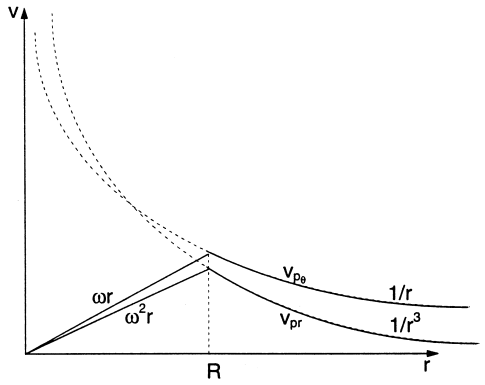

Figure 16. Particle velocity profiles.

$$\varepsilon^{-q}\frac{\mathrm{d}^2\bar{r}}{\mathrm{d}\bar{t}^2}+\frac{\mathrm{d}\bar{r}}{\mathrm{d}\bar{t}}=\varepsilon^{2m-2p+q}\,\bar{r}\,\dot{\bar{\theta}}^2. \qquad [47]$$

When $q < 0$, $2s + p - m = 0$, $2m - 2p + q = 0$, the result is $2s = m - p = -q/2 > 0$, i.e. $\varpi = \Omega\tau_v < 1$. In this particular case, to which the analysis is restricted here with $l_{\mathrm{ref}} = L = r_v$, the solution is:

$$\begin{aligned}\dot{\theta}&=\varpi, \quad \dot{r}=\varpi^2 r, \quad r\leq R\\ \dot{\theta}&=\frac{1}{r^2}, \quad \dot{r}=\frac{1}{r^3}, \quad r\geqslant R\end{aligned} \qquad [48]$$

For this particular case, the particle velocity profiles are given in figure 16. The asymptotic solution [48] obtained for small rotation velocities (or small values of τ_v or both) is steady.

The particle trajectories differ according to the particle initial position. A particle coming from $r = a < R$ at $t = 0$ has one trajectory equation up to $r = R$; this equation then changes for $r > R$. A particle located outside the solid disk at the initial time has a single trajectory equation.

This behavior can be seen with the concentration curves, assuming the concentration to be uniform at the initial time (figure 17). The three above regions appear very clearly (Dodemand, 1994) at the different times. It is interesting to compare these results with those of figure 13.

In the case of the modified Rankine vortex, the solution is numerical. The asymptotic behavior give the same results as those of the Rankine vortex.

4. CONCLUSION

An analysis of particle trajectories in a suspension carried by a vortex has been performed for vorticity concentrated in a point (irrotational vortex). Using the description of the suspension in Lagrangian coordinates, it has been shown that the various possible steady and unsteady solutions and each situation have been related to a physical situation. This approach appeared necessary because of the difficulty in interpreting certain results and behaviors. The concepts of continuum and discontinuity were mentioned. Partial particle density (or concentration) profiles were plotted for the different cases. The results were then interpreted in Eulerian coordinates. Finally, the investigation of the simple and modified Rankine vortices has been performed without going as far as for the singular vortex. In each case, it was assumed that the usual assumptions for dilute suspensions were verified.

Although laminar vortices do exist, including in combustion, it is generally for only very short times. Nevertheless, in complex fluid flows, it is interesting to use models easier to interpret. The work carried out here utilizes such simple fluid flow configurations which are frequently used to analyze interaction phenomena: vortex diffusion (Germain, 1986), diffusion

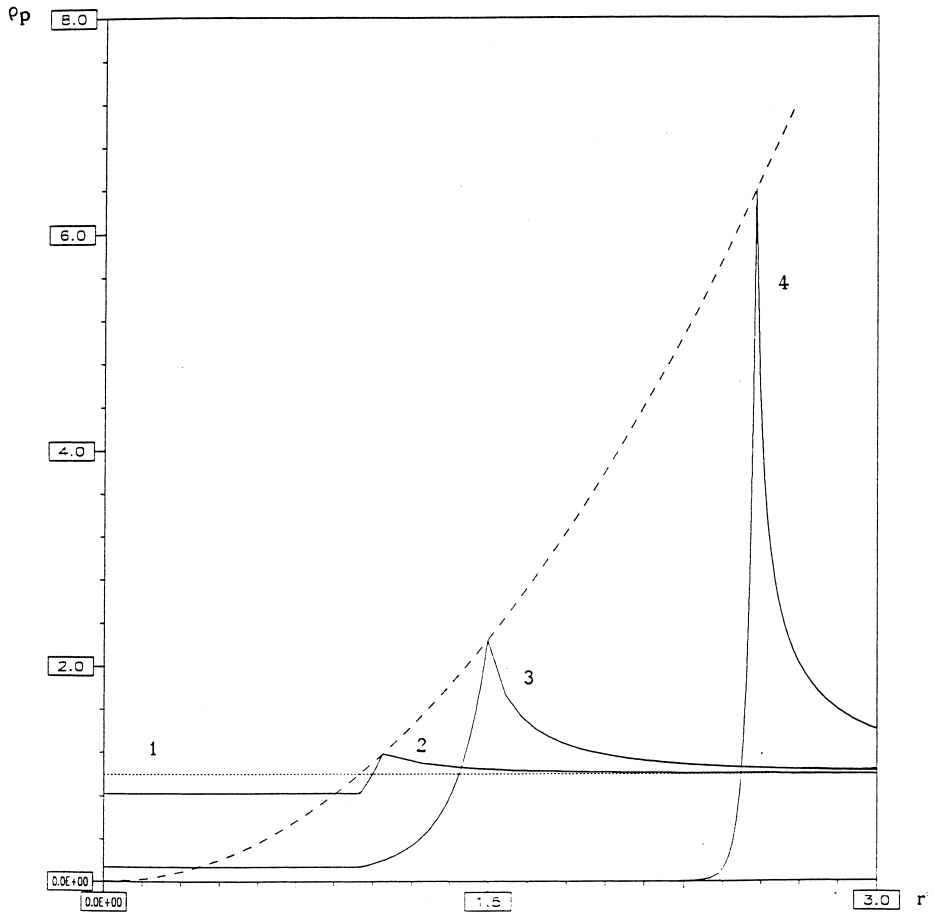

Figure 17. Particle density versus vector radius $\rho_p(a,0) = 1$, $\bar{m} = 0.1 \ll 1$. 1: $t = 0$, 2: $t = 1$, 3: $t = 10$, 4: $t = 100$.

flame and premixed flames (Marble, 1985; Marble, 1988; Rangel and Continillo, 1992; Fichot *et al.*, 1993).

Heat transfer would have to be taken into account in order to generalize this theory, as do evaporation and condensation when it applies to droplets and combustion.

It should be noted that Tio and Lasheras are also investigating the motion of a particle in a Stuart vortex (Stuart, 1967; Gañán-Calvo and Lasheras, 1991; Tio and Lasheras, 1993; Lasheras and Tio, 1994) in gravity. The Stuart vortex street actually corresponds to a succession of modified Rankine vortices. The fluid streamlines have the appearances of cat eyes. In the presence of gravity some stable and unstable configurations are observed. Also experimental measurements made recently by Isaacson (1993) show that the velocity profiles obtained from the analytic expression of the Stuart vortex stream function agree perfectly with the velocity profiles measured in certain shear layers.

The study of asymptotic particle behaviors in a Stuart vortex would require the use of a system of orthogonal curvilinear coordinates related to the fluid, in order to proceed as above. This is possible, but complex, and the results would certainly be limited.

Marcu *et al.* (1995) have analyzed the behavior of particles in a Burgers vortex which is a three dimensional flow. An asymptotic analysis would certainly be interesting here too.

REFERENCES

Burgess, J. M. (1948) A mathematical model illustrating the theory of turbulence. *Adv. Appl. Mech.* **1,** 171.

Gañán-Calvo, A. M. and Lasheras, J. C. (1991) The dynamics and mixing of small spherical particles in a plane, free shear layer. *Phys. Fluids A* **3**, 1207–1217.

Clift, R., Grace, J. R. and Weber, M. E. (1978) *Bubbles, Drops and Particles*. Academic Press, New York.

Delery, J., Barberis, D. and Molton, P. (1997) Physique du décollement tridimentionnel et formation de tourbillons. *Colloque ONERA*. Centre des Congrès de la Villette, Paris.

Dodemand, E. (1994) Comportement d'une suspension en présence d'ondes acoustiques et de tourbillons. Thèse de doctorat de l'Université de Valenciennes.

Dodemand, E., Prud'homme, R. and Kuentzmann, P. (1995) Influence of unsteady forces acting on a particle in a suspension. Application to the sound propagation. *Int. J. Multiphase Flow* **21**, 27–51.

Dodemand, E. and Prud'homme, R. (1991) Comportement d'une suspension en présence d'un tourbillon irrotationnel *10ème Congrès Franç*ais de Mécanique Université de Jussieu—Paris.

Fichot, F., Harstad, K. and Bellan, J. (1993) Unsteady evaporation and combustion of a drop cluster inside a vortex. *31st Aerospace Sciences Meeting & Exhibition*, Reno, NV AIAA 93-0695.

Fortier, A. (1967) *Mécanique des suspensions*. Masson & Cie.

Germain, P. (1962) *Mécanique des milieux continus*. Masson.

Germain, P. (1986) *Mécanique*—Tome 1 Ecole Polytechnique Ellipses.

Guyon, E., Hulin, J. P. and Petit, L. (1991) *Hydrodynamique physique*. Savoirs actuels Inter Editions/Editions du CNRS.

Isaacson, L. V. K. (1993) A deterministic prediction of ordered structures in an internal free shear layer. *J. Non-Equilib. Thermodyn.* **18,** 256–270.

Kuentzmann, P. (1973) Aérothermochimie des suspensions, *Mémoires de Sciences Physiques. Fascicule 72*, Gauthier–Villars.

Lasheras, J. C. and Tio, K. K. (1994) Dynamics of a small spherical particle in steady two-dimensional vortex flows. *Appl. Mech. Rev.* **47**, S61–S69.

Marble, F. E. (1985) Growth of a diffusion flame in the field of a vortex, *Recent Advances in Aerospace Sciences*, ed. C. Casci, pp. 395–413.

Marble, F. E. (1988) Mixing, diffusion and chemical reaction of liquids in a vortex field, *Colloque International sur la Chimie des liquides*, Paris.

Marcu, B., Meiburg, E. and Newton, P. K. (1995) Dynamics of heavy particles in a Burger vortex. *Phys. Fluids* **7**, 400–410.

Maxey, M. R. and Riley, J. J. (1983) Equation of motion for a small rigid sphere in a nonuniform flow. *Phys. Fluids* **26,** 883–889.

Nigmatulin, R. I. (1991) *Dynamics of Multiphase Media*. Hemisphere, Washington, DC.

Rangel, R. H. and Continillo, G. (1992) Theory of vaporization and ignition of a droplet cloud in the field of a vortex. The 24th International Symposium on Combustion. University of Sydney, Australia.

Soo, S. L. (1990) *Multiphase Fluid Dynamics*, Science Press & Gower Technical.

Stuart, J. T. (1967) On finite amplitude oscillations in laminar mixing layers. *J. Fluid Mech.* **29**, 417–444.

Tio, K. K. and Lasheras, J. C. (1993) The dynamics of a small spherical particle in steady, two-dimensional vortex flows AIAA-93-1874 University of California, San Diego La Jolla, California AIAA/SAE/ASME/ASEE 29th Joint Propulsion, Conference and Exhibit, Monterey, CA.

Tio, K. K., Liñan, A., Lasheras, J. C. and Gañán-Calvo, A. M. (1993a) On the dynamics of buoyant and heavy particles in a periodic Stuart vortex flow. *J. Fluid Mech.* **254,** 671–699.

Tio, K. K., Gañán-Calvo, A. M. and Lasheras, J. C. (1993b) The dynamics of small, heavy, rigid spherical particles in a periodic Stuart vortex flow. *Phys. Fluids A* **5**, 1679–1692.

APPENDIX A

Pressure Gradient And Virtual Mass Effects

For a small spherical particle in an unsteady flowfield, the momentum equation can be written (Maxey and Riley, 1983; Tio *et al.*, 1993a,b; Dodemand *et al.*, 1995):

$$\frac{4}{3}\pi r_p^3 \rho_{ps} \frac{d_p \mathbf{v}_p}{\mathrm{d}t} = 6\pi\mu r_p f_p(\mathbf{v}_g - \mathbf{v}_p) + \frac{2}{3}\pi r_p^3 \rho_{gs}\left(\frac{d_g \mathbf{v}_g}{\mathrm{d}t} - \frac{d_p \mathbf{v}_p}{\mathrm{d}t}\right) - \frac{4}{3}\pi r_p^3 \mathbf{grad}(p) + \frac{4}{3}\pi r_p^3 \rho_{ps}\boldsymbol{g} + \boldsymbol{F}_\mathrm{l} + \boldsymbol{F}_\mathrm{b}, \tag{A1}$$

where r_p is the particle radius, $\mathbf{v}_g$,$\mathbf{v}_p$ and $(d_p\mathbf{v}_p)/(\mathrm{d}t)$ have been defined previously, $(d_g\mathbf{v}_g)/(\mathrm{d}t)$ is the local fluid acceleration, ρ_{gs} and ρ_{ps} are the gas and particle densities, μ is the fluid viscosity, f_p is a coefficient correcting for the effects of non-zero Reynolds, p is the local pressure, $\boldsymbol{g}$ is the gravitational acceleration, $\boldsymbol{F}_\mathrm{l}$ is the lift and $\boldsymbol{F}_\mathrm{b}$ is the Basset history force.

The gravity term will not be taken into account for two-dimensional horizontal vortices. The last two forces will be neglected for simplicity.

Writing the momentum equation of the fluid, inviscid and at constant density, and subtracting from [A1], one obtains:

$$\frac{4}{3}\pi r_p^3(\rho_{ps} + 0.5\rho_{gs})\frac{d_p \mathbf{v}_p}{\mathrm{d}t} = 6\pi\mu r_p f_p(\mathbf{v}_g - \mathbf{v}_p) + 2\pi r_p^3 \rho_{gs}\frac{d_g \mathbf{v}_g}{\mathrm{d}t}. \tag{A2}$$

This equation contains implicitly the effects of virtual mass and pressure gradient.

With

$$\tau_v = \frac{2\rho_{ps} r_p^2}{9\mu f_p(1 - 0.5E)},\ E = \frac{\rho_{gs}}{\rho_{ps} + 0.5\rho_{gs}}, \tag{A3}$$

the fluid density is assumed to be very small compared with the specific density of the particle and the ratio E is then very small. Then the last term of the final relation of the problem [A2] is generally negligible, except for very strong accelerations of the fluid. This is the case in the vicinity for the vortex center with concentrated vorticity. This is also the case for high rotational velocity Rankine vortices. The central force due to the fluid pressure gradient becomes higher than the radial component of the particle acceleration.

For a vortex with concentrated vorticity, reference quantities defined in [8] are valid and the following equation is obtained instead of [9]:

$$\frac{d_p \mathbf{v}_p}{\mathrm{d}t} = \frac{1}{r}\mathbf{e}_\theta - \mathbf{v}_p - \frac{3E}{2r^3}\mathbf{e}_r. \tag{A4}$$

If r and θ are the particle radial and tangential coordinates, one has:

$$\frac{1}{r}\frac{\mathrm{d}(r^2\dot{\theta})}{\mathrm{d}t} = \frac{1}{r} - r\dot{\theta}, \tag{A5}$$

$$\ddot{r} - r\dot{\theta}^2 = -\dot{r} - \frac{3E}{2r^3}, \tag{A6}$$

and using the definitions [12], [13] and [14] are replaced by:

$$r^2\dot{\theta} = 1 + (a^2\beta - 1)e^{-t}, \tag{A7}$$

$$\ddot{r} + \dot{r} = \frac{[1 + (a^2\beta - 1)e^{-t}]^2 - 1.5E}{r^3}. \tag{A8}$$

[A6] shows that the term in E becomes significant when:

$$|r^2\dot{\theta}| \approx \text{ or } \langle\sqrt{1.5E}. \tag{A9}$$

Using [115] and putting:

$$E = \varepsilon^{\rho} \tag{A10}$$

for studying the asymptotic behavior of the system, one finds that the only case of interest will be case I of table 1 (which is modified):

$$q \geqslant m + p > 0 \tag{A11}$$

and we find that the effect of E is not negligible when:

$$4p - 2q = \rho \tag{A12}$$

That means:

$$\frac{r^2}{t} = O(\sqrt{E}) \tag{A13}$$

Figure A1 shows the numerical results obtained for $K = a^2\beta = 0$ and E equal to 10^{-1} and 10^{-3}. In the last case and for $E < 10^{-3}$ it is evident that the influence of E is non negligible only for very small values of r. The case $K = 0$ corresponds to a vortex suddenly introduced into a suspension at rest. The particles which are sufficiently near the vortex center move toward this center before going away, because they are carried in rotation by the fluid vortex, with increasing values of r.

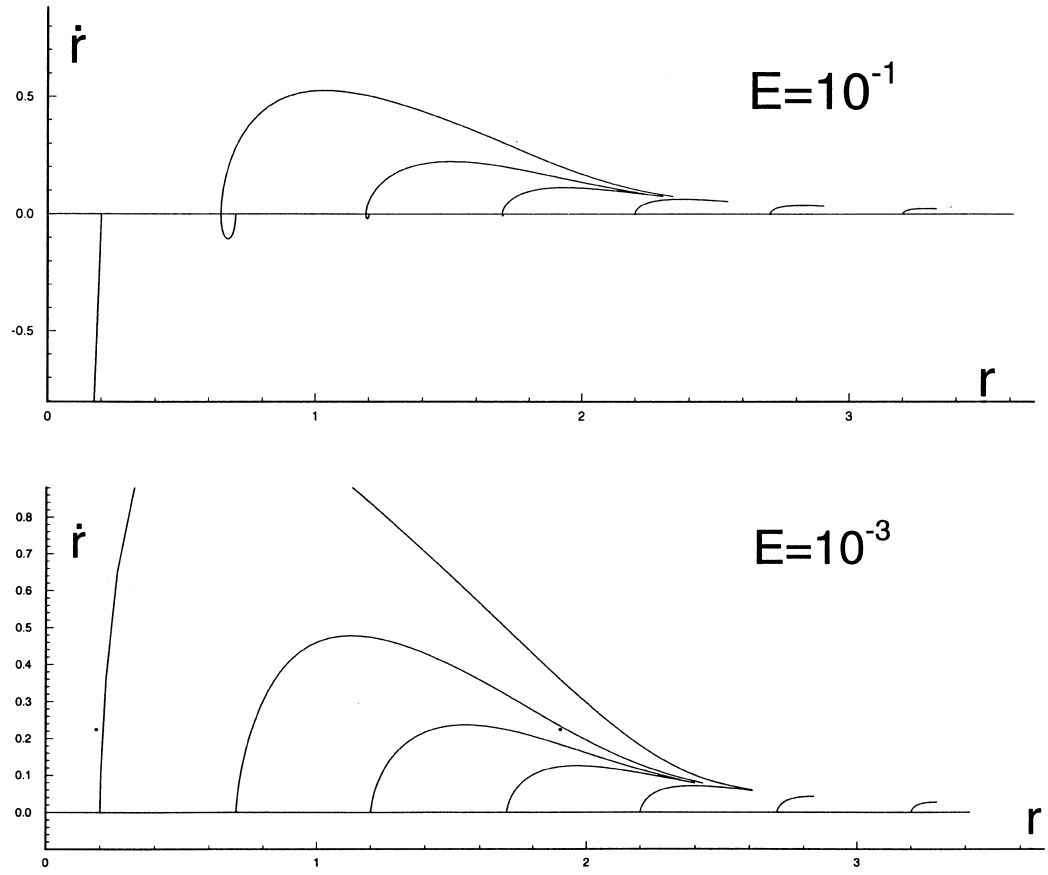

Figure A1. Particles at rest at the initial time, $b(a) = 0$, $\beta(a) = 0$ (or $K = 0$). Influence of the gas/particles density ratio $E = \rho_{gs}/(\rho_{ps} + 0.5\rho_{gs})$.